Synthesis and Characterization of Poly(acrylonitrile)/Montmorillonite Nanocomposites from Surface-Initiated Redox Polymerization

Chao-Yen Chen, Chi-Chang Chen, Sheng-Shu Hou

Department of Chemical Engineering, National Cheng Kung University, Tanian 70101, Taiwan

Received 15 July 2008; accepted 11 June 2009
DOI 10.1002/app.31022
Published online 1 September 2009 in Wiley InterScience (www.interscience.wiley.com).

ABSTRACT: We have developed a facile method to prepare polyacrylonitrile/montmorillonite (PAN/MMT) nanocomposites using the surface-initiated redox polymerization of acrylonitrile (AN) in the aqueous phase. The MMT silicate surfaces were first treated with diethanolamine, and the modified MMT (DEA-MMT) was subsequently used together with the Ce(IV) salt to serve as a redox system. The PAN chains growing on a surface-tethered DEA expand the interlayer space, and thus lead to intercalated/exfoliated nanocomposites. The nanomorphology of the prepared nanocomposites depends on the AN/OH molar ratio in feed. An exfoliated PAN/MMT nanocomposite was obtained when the feeding AN/OH molar ratio = 300 was used. The molecular weight of PAN in the nanocomposites prepared by the present method is also dependent on the AN/OH molar ratio in feed and can be up to ca. 160,000 g/mol. The differential scanning calorimeter (DSC) and thermogravimetric analysis (TGA) analyses show that the increasing fraction of exfoliated silicate structures should enhance the contact interface between the silicate and polymer, resulting in the higher glass transition temperature and thermal stability. J Appl Polym Sci 115: 416–423, 2010

Key words: polyacrylonitrile; nanocomposite; redox polymerization; diethanolamine

INTRODUCTION

Polymer/layered silicate nanocomposites (PLSNs) composed of inorganic layered silicates (clay) dispersed in the polymer matrix have attracted extensive interest in the past two decades.[1–7] In addition to fundamental researches, applications of PLSNs in engineer materials and commodities have been growing rapidly. Montmorillonite (MMT)-type clay (MMT) is among the most used silicate, because its high aspect ratio yields superior mechanical and physical properties.[2] To enhance compatibility between the hydrophobic polymer and hydrophilic silicate, organophilic modification of the silicate has been needed. The organophilicity of layered silicates usually is attained via cation exchange of intergallery cations by alkylammonium surfactants.

There are two major processes for mass production of PLSNs. The first one is the direct polymer-melt blending of which the organophilic silicate is mixed with the molten polymer at an elevated temperature above the glass transition temperature (T_g) or melting temperature (T_m) of the polymer. PLSNs prepared from melt blending have encountered some inherent difficulties in the preparation and subsequently processing as the amount of silicate loading increases. Except for some successful cases,[8] only a few weight percent loading of clay (<10 wt % at the most)[9,10] can be actually incorporated into the polymer matrix by melt blending.

The other process is the *in situ* intercalative/exfoliative polymerization. This method involves dispersion of the silicate in the monomer solutions followed by their polymerization to produce PLSNs. To synthesize the vinyl polymer-based PLSNs through radical polymerization, one strategy for the *in situ* polymerization is to functionalize the silicate surface with an initiator, which is suitable for the following radical polymerization of the vinyl monomer. Because the polymer chain is tethered directly to the silicate layer, incompatibility between the organic polymer and inorganic silicate could be significantly minimized. In addition, the problems caused by small molecules, such as lowering the thermal stability, reinforcing efficiency, and durability of the polymer nanocomposites, could also be eradicated. Some vinyl polymer-based PLSNs prepared by *in situ* polymerization through an anchored initiator, including controlled/living radical polymerization, have been reported.[11,12]

Polyacrylonitrile (PAN) is a polymer having versatile applications. PAN is now in widespread use for

Correspondence to: S.-S. Hou (sshou@mail.ncku.edu.tw).
Contract grant sponsor: National Science Council of Taiwan; contract grant number: NSC92-2216-E-006-045.

fiber-spinning, electrospinning of nanofibers, and as the precursor of carbon fibers, etc. Furthermore, acrylonitrile (AN) can be easily copolymerized with other vinyl monomer, and thus the resulting copolymers may be used as plastic resins, fibers, or rubbers. PLSNs have been developed for more than two decades; however, it was not until recently that more researches of the PLSNs based on PAN were carried out.[13–19] Most of the PAN-based PLASNs were prepared first by intercalating the initiator into the silicate gallery, and *in situ* polymerization subsequently was conducted. Chung and coworks[13–15] have reported *in situ* polymerization of AN in the presence of silicate (MMT). In their approaches, a combination of 2-acrylamido-2-methyl-1-propanesulfonic acid (AMPS) and thermal-sensitive potassium persulfate (KPS) was used as the initiating system to polymerize the intercalated AN monomers at 65°C. They suggested a complicated mechanism like redox cocatalysis, by which the attached AMPS on the silicate surface would oxidize Fe^{2+} in the silicate lattice to Fe^{3+}, and thus generating radicals for the corresponding polymerization.

In this study, we report a facile method for preparing the PAN/MMT nanocomposites by the polymerization initiated Ce(IV)/ROH redox system, which has been proven effective in the synthesis of block and graft copolymers.[20–24] The synthetic strategy (Scheme 1) is first to functionalize the silicate surface with diethanolamine (DEA). Free radicals were produced by the oxidation of the terminal hydroxyl groups of DEA molecules bounded on clay surfaces by Ce(IV) salt. The polymerization of AN thus can be achieved using the redox system consisting of the Ce((IV) ions and silicate-anchored DEA. Compared with the thermal unstable initiator adsorbed on silica surface,[15] the advantage of using Ce(IV)/DEA redox couple to prepare PLSNs is the stability of DEA, which is easy-processed and thermal nonsensitive to suppress side reactions such as homogeneous polymerization outside the silicate galleries. Moreover, the low-temperature redox polymerization of vinyl monomers is of importance, especially from the economic viewpoint.[25]

EXPERIMENTAL

Materials

Sodium MMT was purchased from Southern Clay Products Inc., and had 92.6 meq/100 g of cation exchange capacity (CEC). AN, DEA, and lithium chloride were purchased from Fluka and used as received. Cerium ammonium nitrate (Ce(IV) salt) and ammonium ferrous sulfate hexahydrate were purchased from SHOWA. The Ce(IV) salt was dried in a vacuum oven under 105°C for 1 h prior to use. Hydrochloric acid (HCl), nitride acid (HNO_3), and *N*,*N*-dimethyl formamide (DMF) were purchased from Adrich and used as received.

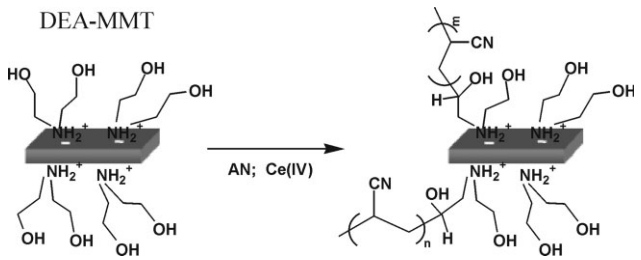

Scheme 1 Illustration of the surface-initiated redox polymerization of acrylonitrile.

Synthesis of DEA-MMT

MMT (1.00 g, 0.926 meq/g) was placed in a 250 mL flask and dispersed vigorously in 100 mL of deionized water at room temperature overnight. DEA was protonated by HCl in water and then was added to the MMT dispersion. The mixture was then stirred for additional 24 h. In this study, excess protonated DEA (five times CEC) were fed to prepare the DEA-modified MMTs, DEA-MMT. The DEA-MMT suspension was filtered and then redispersed in 100 mL of deionized water to remove the unexchanged DEA. This procedure was repeated three times until the water from centrifugation was free of chloride ion by testing with silver nitrate. The exchanged sodium content of filtrate was measured by inductively coupled plasma (ICP) experiment.[26] The amount of DEA-exchanged sodium ion from MMT was determined to be 0.917 meq/g, which meant that 99% of interlayer cations of MMT were exchanged.

Synthesis of MMT/PAN nanocomposites

Five nanocomposites (60m-MMT, 100m-MMT, 160m-MMT, 200m-MMT, and 300m-MMT) were synthesized by the surface-initiated redox polymerization. The number ahead "MMT" represents the feeding molar ratio of AN to the hydroxyl group of DEA, for instance 60m indicates AN/OH molar ratio = 60. All polymerizations were carried out within the solubility range of AN in water. The desired stoichiometric amount of AN was added into the DEA-MMT slurry (0.20 g DEA-MMT in 40 mL deionized water) in a 250 mL four-necked flask under nitrogen atmosphere. The solution was stirred at room temperature and then the Ce(IV) salt (0.21 g, 0.38 mol) in 0.10 *N* HNO_3 solution was added dropwise in 20 min. After completion of this addition, the mixture was stirred for another 6 h in the absence of light. The reaction was stopped by adding excess amount of ferrous

TABLE I
The Reactant Compositions for Redox Polymerization

Samples	Reactants for redox polymerization: DEA-MMT (g)	AN (g)	AN (wt %)[a] in feed	Feeding molar ratio of AN/OH	Organic content in the nanocomposite[b] (wt %)
60m-MMT	0.20	1.20	85.7	60	47.7
100m-MMT	0.20	2.00	90.9	100	74.7
160m-MMT	0.20	3.20	94.1	160	87.5
200m-MMT	0.20	4.00	95.2	200	94.0
300m-MMT	0.20	6.00	96.7	300	97.0
200m-PAN[c]	–	2.1	4	200	–

[a] The weight percentage of AN in feed is calculated as AN/AN + DEA-MMT.
[b] Organic encapsulation was determined by TGA in air.
[c] The control sample which was prepared without adding DEA-MMT.

ammonium sulfate into the reaction mixture, while all the unreacted Ce(IV) ions were reduced to Ce(III) ions.[23] The crude product was allowed to precipitate and collected by centrifugation. The product was washed with water several times to remove the unreacted AN and metal ions.

Characterizations

To analyze the molecular weight of PAN, the surface-anchored PAN was extracted as follows: 0.20 g of the dried nanocomposite was extracted with LiCl/DMF (0.20 g/ 60 mL) solution under a nitrogen atmosphere at 80°C for 5 days. The mixture was centrifuged to separate dissolved PAN from the layered silicates. The extract was filtered to remove suspended silicates, and then poured into a large amount of methanol to precipitate PAN. The precipitated polymer was dried under vacuum at 60°C for 48 h before conducting the measurement of the molecular weight. The weight average molecular weight, M_w, was obtained by determining the intrinsic viscosity ([η]) of extracted PAN in DMF 25°C with a Cannon-Fenske capillary viscometer. The M_w were calculated by using the following relationships[27,28]:

$$[\eta] = \frac{\eta_{sp}/c}{1 + 0.28 \times \eta_{sp}}$$

$$[\eta] = 2.33 \times 10^{-4} \times M_w{}^{0.75}$$

where [η], η_{sp}, and c are the intrinsic viscosity, specific viscosity, and concentration (fixed at 0.2 g/dL), respectively.

X-ray powder diffraction (XRD) was performed on a Rigaku RINT2100 X-ray diffractometer with CuKα radiation (λ = 0.1524 nm) operated at 40 kV and 30 mA in the two-theta range of 2° to 25°. Transmission electron microscopy (JEOL TEM 1200-EX electron microscope operated at 80 kV) was used to examine the morphology of nanocomposites. The dried nanocomposite samples were embedded in epoxy resin and cured at 65°C for 24 h and then sectioned by ultramicrotome to a thickness of 30 nm. Infrared spectra were recorded at 4 cm^{-1} resolution on a Fourier transform infrared spectrometer (FTIR, Nicolet5700) in the region of 400 to 4000 cm^{-1}. Samples used were thin films coated on potassium bromide (KBr) pellet. The thermal stability of PAN and organic encapsulation in the nanocomposite were determined with a thermogravimetric analyzer (TGA, Perkin-Elmer TGA7) over a temperature range of 50–700°C at a heating rate of 30°C/min in air.[29] Differential scanning calorimeter (DSC, DuPont TA2010) measurements were conducted over the temperature ranges of 10–150°C at a heating rate of 10°C/min under dry nitrogen atmosphere. The inflection point of the DSC thermogram was taken as the glass transition temperature (T_g) of the sample.

RESULTS AND DISCUSSION

Surface-initiated redox polymerization of acrylonitrile in the presence of DEA-MMT

Scheme 1 illustrates the surface-initiated redox polymerization of the intercalated AN monomers in the galleries of DEA-MMT. Similar to the conventional method for preparing organosilicates using cationic surfactants, in this study diethanol ammonium chloride acts like the surfactant and is used for the preparation of DEA-modified MMT (DEA-MMT). The surfaces of modified silicate layers are thus cover with diethanol functional groups. The degree of ion exchange is 99% on the basis of ICP analysis, which determines the Na^+ concentration of the filtrated solution after the ion exchange.

Table I summarizes the reactant compositions for the surface-initiated redox polymerization of AN in the presence of DEA-MMT. The weight of loading DEA-MMT is kept the same and AN/OH molar ratio

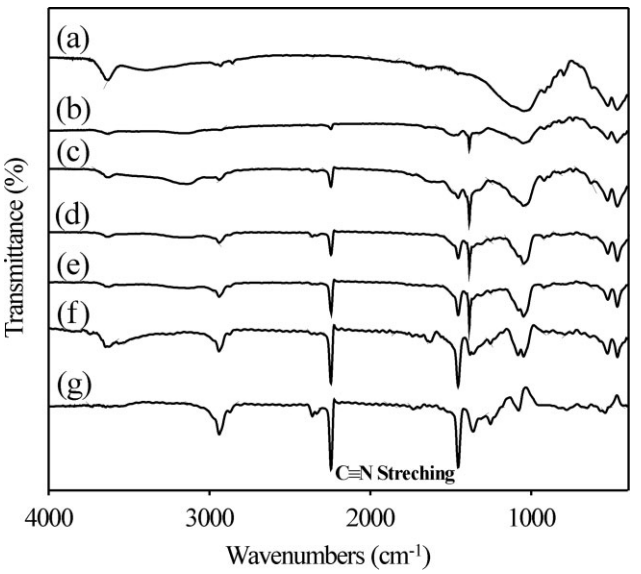

Figure 1 The FTIR spectra of (a) DEA-MMT and PAN/MMT nanocomposites, (b) 60m-MMT, (c) 100m-MMT, (d) 160m-MMT, (e) 200m-MMT, and (f) 300m-MMT, and (g) the spectrum of the control sample 200m-PAN.

varies from 60 to 300 for five samples. The Ce(IV)/OH molar ratio is 1/1 for all the polymerizations. In the process of redox initiation, Ce(IV) ion is reduced with the abstraction of one hydrogen from the methylene carbon next to the hydroxyl group,[21–23] and the carbon-centered radical is the primary initiating point for polymerization of AN. Note that the neat DEA-grafted polyacrylonitrile (200m-PAN, with the feeding molar ratio of AN/OH = 200) was prepared without addition of DEA-MMT as the control sample for the purpose of comparison. Furthermore, when diethylamine-modified MMT was used instead of DEA-MMAT, no polymer formed within 6 h under the same reaction conditions. This control experiment conforms that the polymerization of AN is indeed initiated by the combination of Ce(IV) and surface-anchored OH of DEA-MMT.

Figure 1 shows the FTIR spectra of DEA-MMT, 200m-PAN, and PAN/MMT nanocomposites. The spectra (b)–(f) contain all the characteristic absorbance bands of PAN and MMT, indicating that the PAN/MMT nanocomposites have been successfully prepared. The bands of 2927 and 2864 cm^{-1} are due to the asymmetric and symmetric C—H stretching vibration. Additionally, C≡N stretching at 2237 cm^{-1}, CH_2 and C—H bending at 1447 and 1310 cm^{-1}, and the peaks of 1359 (CH_2 wagging) and 1247 cm^{-1} (C—H wagging) are the characteristic absorbance bands of PAN.[30] The characteristic peaks originated from MMT can be found at 3626 cm^{-1} for the silicate OH group,[31–33] about 1041 cm^{-1} for Si—O stretching, and at 522 cm^{-1} for Si—O bending.

The effectiveness of the surface-initiated polymerization of AN depends on the AN/OH molar ratio in feed and can be evaluated by the organic encapsulation in the final nanocomposites, as listed in Table I. For the 60m-MMT sample (AN/OH = 60), the organic encapsulation in the final nanocomposite is only 47.7 wt %, whereas AN in feed is 85.7 wt %. In contrast, the content of organic encapsulation for 200m-MMT and 300m-MMT is almost the same to the corresponding content of AN in feed. These results indicate that polymerization of AN occurs mainly in the silicate galleries. As the polymerization is initiated on the silicate surfaces, the silicate galleries become hydrophobic because of occupation of PAN chains therein. During the course of polymerization, AN will diffuse into the silicate galleries and therefore the polymer chain can grow up. More amount of AN in feed means that more AN can diffuse into the silicate galleries and then be polymerized. Thus, the organic content and average molecular weight (M_w) of PAN (Table II) formed in the presence of DEA-MMT increase with increasing AN/OH molar ratio in feed. The M_w of PAN increases on increasing the amount of AN in feed as keeping all other factors constant, which is in accordance with the reported observations in the

TABLE II
Characterization of PAN/MMT Nanocomposites

Samples	*d*-spacing (nm)	T_g (°C)	$T_{0.1}$ (°C)[a]	$T_{0.1\text{-org}}$ (°C)[b]	M_w of extracted PAN
MMT	1.28	–	–		–
200m-PAN[c]	–	87	373	373	200,700
60m-MMT	2.01	–	255	226	31,200
100m-MMT	No peaks	92	309	272	61,100
160m-MMT	No peaks	93	362	360	100,200
200m-MMT	No peaks	97	367	367	138,600
300m-MMT	No peaks	100	380	380	158,900

[a] $T_{0.1}$ is the temperature of initial 10% weight loss of nanocomposites.
[b] $T_{0.1\text{-org}}$ is the temperature of initial 10% weight loss of the organic component in the nanocomposite.
[c] The control sample which was prepared without adding DEA-MMT.

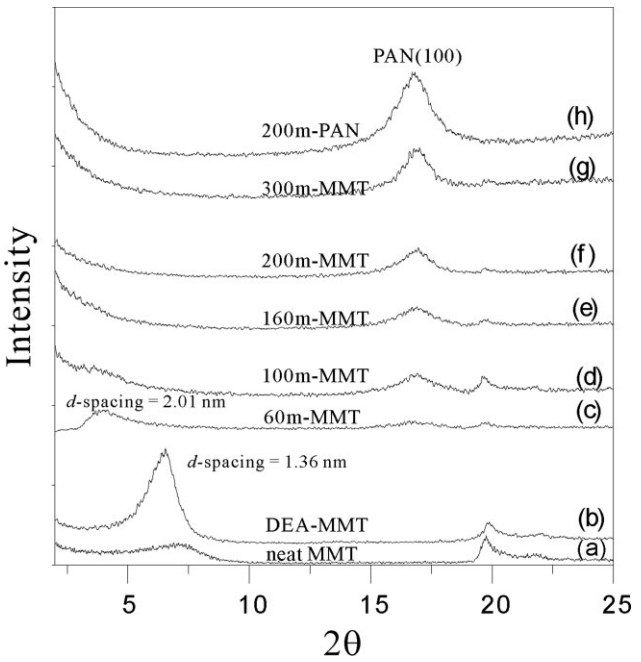

Figure 2 X-ray diffraction patterns of (a) neat MMT, (b) DEA-MMT, (c) 60m-MMT, (d) 100m-MMT, (e) 160m-MMT, (f) 200m-MMT, (g) 300m-MMT, and (h) 200m-PAN.

similar systems.[23] Furthermore, the high molecular weight of PAN obtained by the Ce(IV)/OH initiation pair (Table II) reflects that the polymer chain is growing on certain OH cites. It should be noted that 200m-PAN has an even higher molecular weight than either the 200m-MMT or 300m-MMT, indicating that the clay platelets hinder the growth of the polymer chains on some of the initiating sites trapped in the middle or center of the platelets.

X-ray diffractograms of the PAN/DEA-MMT nanocomposites

The wide angle X-ray diffractograms of the PAN/DEA-MMT nanocomposites prepared via the polymerization with the Ce(IV)-DEA redox couple are presented in Figure 2, in which the XRD patterns of the parent clay and DEA-MMT are also shown for the purpose of comparison. The neat MMT has a broad peak, which corresponds to an interlayer *d*-spacing of 1.28 nm. The intercalation of DEA into the silicate galleries could be confirmed with the shift of the diffraction peak toward a lower angle value. The DEA-MMT shows a distinct peak (6.28°) corresponding to *d*-spacing of 1.36 nm, and the intensely sharp peak is indicative of a more ordered gallery structure compared to the neat MMT. The XRD pattern of the 60m-MMT nanocomposite reveals a broad diffraction peak at 4.39°, showing a significant increase in the interlayer spacing (2.01 nm). With the feeding ratio of AN to hydroxyl group higher than 100 [diffractograms (d)–(h) in Fig. 2], no more basal (001) peaks are visible for $2\theta < 4°$, indicating the delamination of the MMT layers in the polymer matrix. However, the lack of diffraction peaks in the XRD pattern is not necessary for exfoliation of silicate plates within the nanocomposite. Many factors, such as concentration and order of the clay, can influence the XRD patterns of layered silicates.[33–35] The true nano-morphology of the nanocomposites should be corroborated by TEM analysis.

The diffractogram (h) in Figure 2 for the control sample, pure PAN, presents a sharp intense peak at 16.7°C, the (100) diffraction due to the lateral repeat distance of the hexagonal lattice of PAN.[36,37] As can be seen in Figure 2, the intensity of diffraction peak from PAN crystals increases with PAN loading in the nanocomposites. The increases in crystallinity of PAN are expected and can be attributed to an increased molecular weight of PAN as the higher feeding AN/OH ratio in the preparation of PAN/MMAT nanocomposites.

TEM of the PAN/MMT nanocomposites

Figure 3 shows the TEM micrographs of the PAN/MMT nanocomposites (100m-MMT, 200m-MMT, and 300m-MMT). The images of low magnification reveal that the inorganic silicates are dispersed homogeneously within the polymer matrix. In the images of high magnification, the microtomed sections perpendicular to the basal plane show the layer stacks as thin black strokes. Although the XRD patterns of 100m-MMT and 200m-MMT samples reflect exfoliation of the silicate layers, a mixed nano-morphology composed of the exfoliated and intercalated nanostructures is observed for these two samples. With closely inspection of the right images in Figure 3(a,b), it could be found that some silicate layers are separated far more than 5 nm. Some silicate plates of the 200m-MMT sample are even delaminated as single layers present, as indicated by white arrows. The large interlayer spacing and delamination of the silicate layers account for the invisibility of diffraction peak in XRD patterns. For the 300m-MMT sample [Fig. 3(c)] with the highest organic encapsulation in the nanocomposite, it shows the uniform dispersion of exfoliated silicate layers in the polymer matrix, which is coincided with the result shown by XRD analysis.

Differential scanning calorimetric study of the PAN/MMT nanocomposites

Figure 4 shows the DSC thermograms of the PAN/MMT nanocomposites and the control PAN sample. In all curves of PAN/MMT nanocomposites, the glass transitions are not as obvious as that of

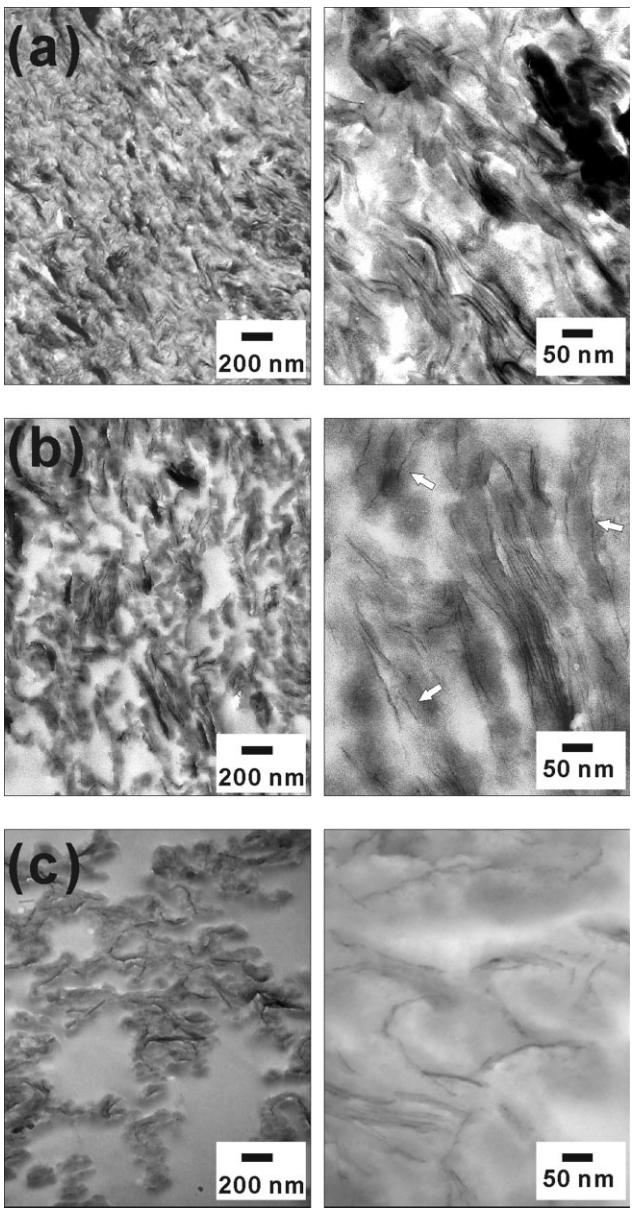

Figure 3 TEM micrographs of PAN/MMT nanocomposites: (a) 100m-MMT, (b) 200m-MMT, and (c) 300m-MMT. The image of higher magnification is shown on the right side. The white arrows in the right image of (b) indicate the delaminated silicate layers.

200m-PAN with the inflection temperature at 87°C, which is assigned to be the T_g of PAN. The slight inflections are observed in the range of 92 to 100°C, and are assigned to be the T_gs of PAN in the PAN/MMT nanocomposites, and the T_g of PAN increases with the increasing AN/OH ratio in feed as listed in Table I. It should be noted that no distinct T_g is found for the 60m-MMT sample. Considering the intercalated structure of the 60m-MMT sample revealed by XRD, it is reasonable that intercalated PAN do not show the characteristic bulk glass transition.[38] Moreover, Wang et al.[39] have also reported that the glass transition peak of intercalated poly(vinyl chloride)/MMT nanocomposites shifted to higher temperatures compared to that of pristine polyvinyl chloride, as a result of the confined environment which restricts the mobility of polymer chains within the interlayers. For the PAN/MMT composites under investigation, XRD and TEM results reveal the intercalated or exfoliated silicate structures. The PAN chains are physically anchored on the clay plates by grafting from intercalated DEA molecules, leading to hinder the movement of the PAN segments. The results of DSC analysis indicate that the increasing ratio of exfoliated silicate structures should increase the contact interface between clay and polymer and hence hindered the transition of PAN chains, resulting in the highest T_g of 300m-MMT.

Thermogravimetric analysis of the PAN/MMT nanocomposites

The thermal stability of PAN/MMT nanocomposites relative to the 200m-PAN (the control sample containing no silicates) has been investigated by TGA in air.[29] The original TGA traces are shown in Figure 5; for comparison, a TGA scan of DEA-MMT which contains no polymer is also included. It should be noted that in Table II two kind of temperature of initial 10% weight loss are calculated on the basis of

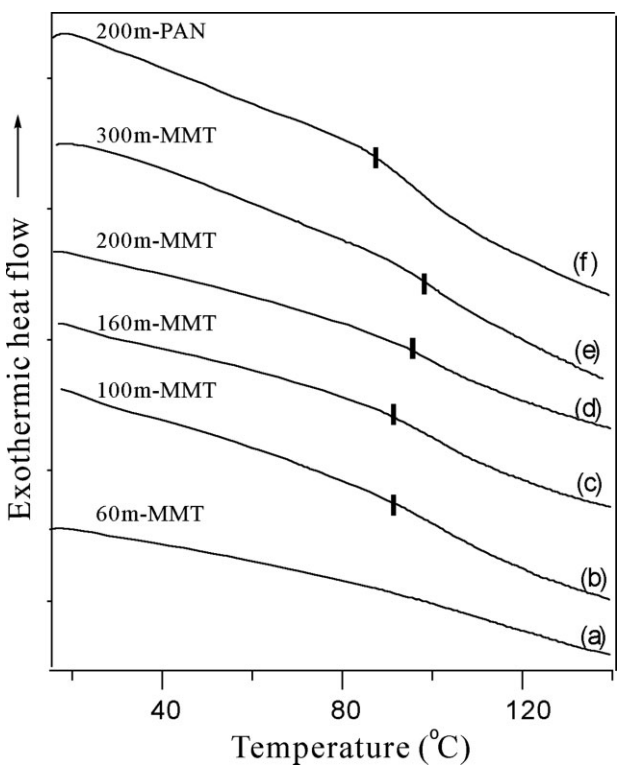

Figure 4 DSC thermograms of (a) 60m-MMT, (b) 100m-MMT, (c) 160m-MMT, (d) 200m-MMT, (e) 300m-MMT, and (f) 200m-PAN. The onset transition temperature as indicated is taken as the glass transition temperature (T_g).

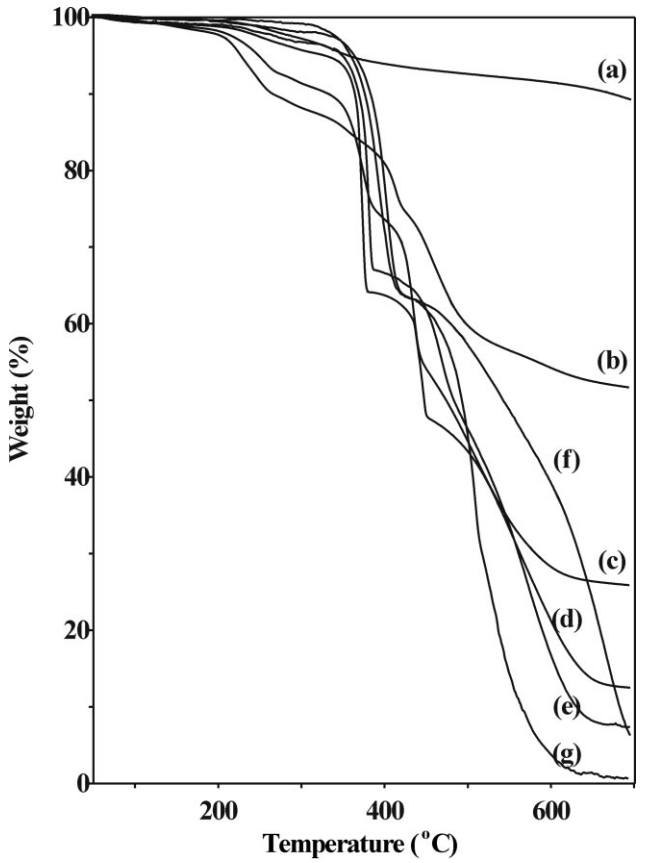

Figure 5 Original TGA traces of (a) DEA-MMT, (b) 60m-MMT, (c) 100m-MMT, (d) 160m-MMT, (e) 200m-MMT, (f) 300m-MMT, and (g) 200m-PAN. The weight loss is calculated on the basis of the total weight of whole nanocomposite sample.

the total weight of nanocomposite sample ($T_{0.1}$) and the organic component ($T_{0.1\text{-org}}$), respectively. The TGA curve of DEA-MMT (trace a) involved the thermal decomposition of the intercalated DEA started at around 200°C.[40] The control 200m-PAN sample (trace g) exhibits two stages of thermal degradation. The first stage of weight loss appears ranging from 350 to 400°C, and the second weight-loss step starts at ca. 450°C.

The 300m-MMT sample, of which the M_w of extracted PAN is comparable to 200m-PAN, also shows two stages of thermal degradation (trace f). For the 300m-MMT sample, the first stage is almost identical to that of 200m-PAN but has a slightly higher $T_{0.1}$ of 380°C. Nevertheless, the rate of weigh loss vs. temperature for 300m-MMT is significantly slower that for 200m-PAN, an indication that 300m-MMT sample possesses better resistance to thermal decomposition, as compared to the 200-PAN sample. Although the 200m-MMT sample contains a more amount of inorganic silicates, 200m-MMT does not offer the expected superior thermal stability over 300-MMT. There are two weight-loss stages for 200m-MMT (trace e); the first stage shifts to a lower temperature range and the $T_{0.1}$ is 367°C, and the decomposition rate in the second stage lies in between those for 200m-PAN and 300m-MMT. The 160m-MMT sample (trace d) degrades in three consecutive steps with the $T_{0.1}$ of 362°C, and the decomposition rate in the final stage is about the same with that of 200m-MMT. The 60m-MMT and 100m-MMT samples (traces b and c) show complex multistages of thermal decomposition at the temperature under 450°C, and the degradation takes place significantly at ca. 250°C, much lower than the other three nanocomposites.

To take into account of the various MMT loadings of the nanocomposites, the original TGA weight loss curve of the nanocomposite samples has been converted to a 100% scale of organic component (shown in Fig. 6). It shows that the 60m-MMT and 100m-MMT samples have much lower thermal stability than the pure polymer 200m-PAN and the other PAN nanocomposites, which could be attributed to poor silicate exfoliation and the much lower molecular weight of PAN.

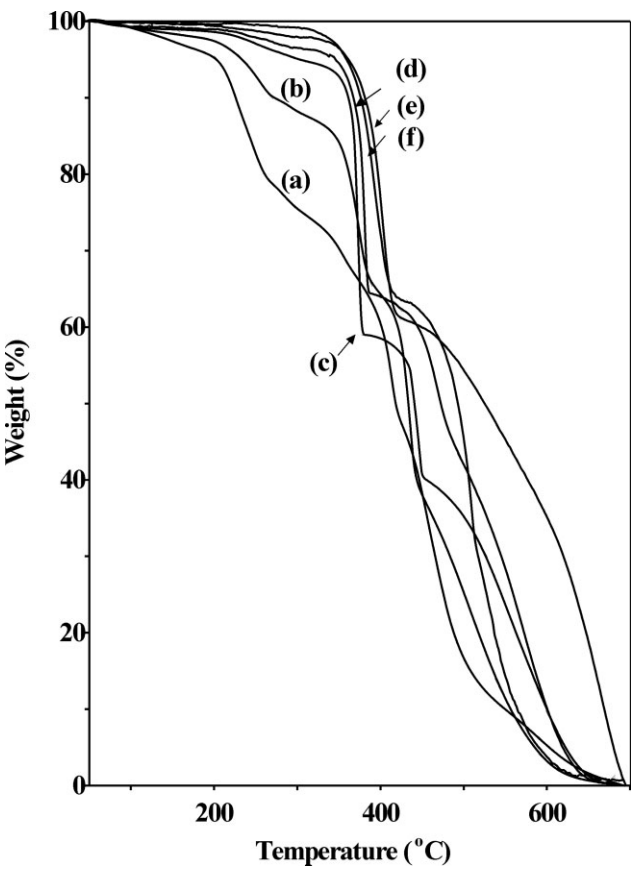

Figure 6 Converted TGA traces of PAN from the corresponding nanocomposites in Figure 5: (a) 60m-MMT, (b) 100m-MMT, (c) 160m-MMT, (d) 200m-MMT, (e) 300m-MMT, and (f) 200m-PAN. The weight loss has been converted to a 100% scale of the organic component.

CONCLUSIONS

The intercalated/exfoliated PAN/MMT nanocomposites were prepared using *in situ* surfacte-initiated redox polymerization of AN in the presence of DEA-MMT. The highly exfoliated nanocomposite (300m-MMT) with higher molecular weight of PAN (M_w = ca. 160,000 g/mol) could have been obtained using higher AN/OH molar ratio (= 300) in feed. However, with decreasing AN/OH molar ratio, only intercalated and intercalated/exfoliated nanocomposites could be achieved. The T_g of the highly exfoliated sample (300m-MMT) is 100°C, 13°C higher than the control PAN sample. The thermal stability is in the order of 300m-MMT $\approx$ 200m-PAN $\approx$ 200m-MMT $\approx$ 160m-MMT $>$ 100m-MMT $>$ 60m-MMT. It is found that the mechanisms of thermal decomposition of 300m-MMT and 200mMMT samples are similar to the pure PAN control sample, showing two stages of thermal degradation. Nevertheless, the degradation rate for the nanocomposites in the second stage is significantly slower than that for the pure PAN control sample.

References

1. Giannelis, E. P.; Krishnamoorti, R.; Manias, E. Adv Polym Sci 1999, 28, 107.
2. Alexandre, M.; Dubois, P. Mater Sci Eng R 2000, 28, 1.
3. Biswas, M.; Ray, S. Adv Polym Sci 2001, 155, 167.
4. Pinnavaia, T. J.; Beall, G. W., Eds. Polymer-Clay Nanocomposite; Wiley: England, 2000.
5. Kickelbick, G. Prog Polym Sci 2003, 28, 83.
6. Qi, R. R.; Jin, X.; Zhou, C. X. J Appl Polym Sci 2006, 102, 4921.
7. Yeh, J.-M.; Liou, S.-J.; Chang, Y.-M. J Appl Polym Sci 2004, 91, 3489.
8. Haraguchi, K.; Ebato, M.; Takehisa, T. Adv Mater 2006, 18, 2250.
9. Usuki, A.; Kojma, Y.; Kawasumi, M.; Okda, A.; Fukushima, Y.; Kurauchi, T.; Kamigaito, O. J Mater Res 1993, 8, 1179.
10. Giannelis, E. P. Adv Mater 1996, 8, 29.
11. Weimer, M. W.; Chen, H.; Giannelis, E. P.; Sogah, D. Y. J Am Chem Soc 1999, 121, 1615.
12. Zhao, H.; Argoti, D.; Farrell, B. P.; Shipp, D. A. J Polym Sci: Part A Polym Chem 2004, 42, 916.
13. Choi, Y. S.; Wang, H. K.; Xu, M.; Chung, I. J. Chem Mater 2002, 14, 2936.
14. Choi, Y. S.; Chung, I. J. Polymer 2003, 44, 8147.
15. Choi, Y. S.; Chung, I. J. Polymer 2004, 45, 3827.
16. Hwang, J. J.; Liu, H. J. Macromolecules 2002, 35, 7314.
17. Fernkndez-Saavedra, R.; Aranda, P.; Ruiz-Hitzky, E. Adv Funct Mater 2004, 14, 77.
18. Yu, T.; Lin., J.; Xu, J.; Chen, T.; Lin, S. Polymer 2005, 46, 5695.
19. Jeong, H. M.; Choi, M. Y.; Ahn, Y. T. Macromol Res 2006, 14, 312.
20. Piirma, I. Polymeric Surfactants; Marcel Dekker: New York, 1992.
21. Nagarajan, S.; Sabdham, K.; Srinivasan, K. S. V. J Polym Sci: Part A Polym Chem 1995, 33, 2925.
22. Nagarajan, S.; Srinivasan, K. S. V. Macromol Rapid Commun 1996, 17, 261.
23. Nagarajan, S.; Kumari, S. S. S.; Srinivasan, K. S. V. J Appl Polym Sci 1997, 63, 565.
24. Al, E.; Güçlü, G.; İyim, T. B.; Emik, S.; Özgümüş, S. J Appl Polym Sci 2008, 109, 16.
25. Bicak, N.; Ozeroglu, C. Eur Polym J 2001, 37, 2393.
26. Chen, C.-C.; Kuo, P.-L. J Colloid Interface Sci 2006, 293, 101.
27. Cleland, R. J.; Stockmayer, W. H. J Polym Sci 1955, 17, 473.
28. Öz, N.; Akar, A.; Yilmaz, N. J Appl Polym Sci 2001, 82, 310.
29. Horrocks, A. R.; Zhang, J.; Hall, M. E. Polym Int 1994, 33, 303.
30. Liang, C. Y.; Krimm, S. J Polym Sci 1958, 31, 513.
31. Hou, S.-S.; Beyer, F. L.; Schmidt-Rohr, K. Solid-State Nucl Magn Reson 2002, 22, 110.
32. Hou, S.-S.; Bonagamba, T. J.; Beyer, F. L.; Madison, P. H.; Schmidt-Rohr, K. Macromolecules 2003, 36, 2769.
33. Chang, C.-C.; Hou, S.-S. Eur Polym J 2008, 44, 1337.
34. Morgan, A. B.; Gilman, J. W. J Appl Polym Sci 2003, 87, 1329.
35. Vaia, R. A.; Liu, W. J. J Polym Sci Part B: Polym Phys 2002, 40, 1590.
36. Pirlot, C.; Willems, I.; Fouseca, A.; Nagy, J. B.; Delhalle, J. Adv Eng Mater 2002, 4, 109.
37. Badawy, S. M.; Sokker, H. H.; Dessouki, A. M. J Appl Polym Sci 2006, 99, 1180.
38. Vaia, R. A.; Ishii, H.; Giannelis, E. P. Chem Mater 1993, 5, 1694.
39. Wang, C.; Qiao, X.; Zhang, Y.; Zhang, Y. X. Polym Test 2003, 22, 453.
40. Ahmed, R.; Nehal, S. Mater Sci Eng A 2005, 399, 368.